Arabian Journal of Geosciences (2020) 13: 39
https://doi.org/10.1007/s12517-019-5010-z

ORIGINAL PAPER

Assessment of water resource carrying capacity based on the chicken swarm optimization-projection pursuit model

Xiang Yu[1] · Jiancang Xie[1] · Rengui Jiang[1] · Ganggang Zuo[1] · Jichao Liang[1]

Received: 19 September 2018 / Accepted: 6 December 2019 / Published online: 7 January 2020

Abstract
Water resource carrying capacity (WRCC) is of great importance to assess the maximum capacity of water resource and scientifically evaluate for sustainable development of economic. This study proposes a chicken swarm optimization-projection pursuit evaluation (CSO-PPE) model, to assess the WRCC of Shaanxi province of China for the period of 2007–2016. The effectiveness of CSO was firstly demonstrated using four typical functions. Then, the CSO-PPM model is used to assess WRCC, and the results were compared with other three algorithms including the particle swarm optimization (PSO), firefly algorithm (FA), and seeker optimization algorithm (SOA). An evaluation index system was established based on the drivers-pressure-state-impact-response-management (DPSIRM) model. The results showed that the WRCC has gradually increased from 2007 to 2016. In addition, the southern and northern regions of Shaanxi province had higher water resource carrying capacity with respect to that of Guanzhong region of Shaanxi province. Additionally, the results also indicated that this evaluation method is feasible for assessing WRCC in Shaanxi province of China, which provide a scientific basis for assessing regional WRCC in other places.

Keywords Water resource carrying capacity · DPSIRM · Projection pursuit evaluation model · Chicken swarm optimization

Introduction

Water resources are essential for the survival and development of humanity, which are also one of the important natural resources for the ecological environment (Varis et al. 2017; Jiang et al. 2018). Water resources determine the economic development of a city and play an important role in the national economy, society, and political issues (Cook and Bakker 2012; Rouillard et al. 2016). The amount of available water resources differs greatly among different countries and regions due to geographical differences. Water resource shortages have become more serious with increasing population and rapid economic development and have limited the sustainable development of economy and society (Jiang et al. 2015; Xing et al. 2019; Jiang et al. 2019). To develop efficient utilization strategies for water resources and to protect the environment, water resource carrying capacity (WRCC) is used to represent the available water resources in a region or basin, to examine whether water resource are sufficient to support the population growth and economic development. The definition of WRCC originated from ecology, which is part of carrying capacity of natural resources (Daily and Ehrlich 1994). The definition of carrying capacity has now been widely used in many fields such as land, urban areas, and sustainable development (Yu and Mao 2002; Graymore et al. 2010; Lane 2010; Wei et al. 2015). Thus, it is essential to scientifically assess the WRCC for better usage of water resources and sustainable development of society and economy.

The system dynamics of WRCC are complex, comprising many characteristics that are mainly changeable, uncertain, and difficult to quantify. Therefore, an index system is needed to reflect the actual situation, and thus provide an accurate evaluation of WRCC. Two methods are mainly used to construct the index system. One method divides the index system into different layers by the levels and factors based on the sustainable development theory (Ren et al. 2016). The other method selects indicators based on the model framework, for instance, the pressure and support (PS), support-pressure-status (SPS), drivers-pressure-state-impact-response (DPSIR), and drivers-pressure-state-impact-response-

Responsible Editor: Broder J. Merkel

✉ Rengui Jiang
jrengui@163.com

[1] State Key Laboratory of Eco-hydraulics in Northwest Arid Region of China, Xi'an University of Technology, Xi'an 710048, China

management (DPSIRM) models (Min et al. 2011; Sun et al. 2016; Zhang et al. 2017; Han et al. 2018). The DPSIRM model has been applied to assess ecological vulnerability, ecosystem health, and the atmospheric environment (Zhang et al. 2016; Zhang et al. 2017; Guo et al. 2018; Li et al. 2019). The DPSIRM model includes different kinds of impact factors pertaining to economy, society, ecology, and environment, which can holistically reflect the interactions among different impact factors. The DPSIRM model highlights coupled relations among water resources, environment, and humans and can strengthen the influence of management strategies.

There are many previous studies focused on the WRCC, e.g., a Florida Keys carrying capacity study was conducted by the State of Florida and the US Army Corps of Engineers (Clarke 2002). Rijsberman and Van de Ven (2000) discussed the assessment of carrying capacities in urban water management. Harris and Kennedy (1999) studied the carrying capacity of agricultural systems at regional level and found that water resources were key limiting factors. Since the 1990s, more studies provided insights into the definition and theory of WRCC and then the characteristics, connotation, and index systems (Mei et al. 2010). Development of numerical methods and models were used to quantitative analyze the WRCC. The representative methods for evaluating WRCC include usual tendency predictions, fuzzy comprehensive evaluation, system dynamics, and principal component analysis (Feng et al. 2008; Gong and Jin 2009). The usual tendency prediction method ignores the connections among factors, and thus cannot provide comprehensive evaluation results. The fuzzy comprehensive evaluation method applies an evaluation matrix to evaluate multiple factors, which solves all kinds of uncertain problems. However, the results are prone to homogenization, discontinuities, distortion, and other issues. The system dynamics method uses computer simulations to build models with complex structures that require massive amounts of data. The principal component analysis method is sensitive to extreme and missing value, which results in inconsistency with fact.

New methods such as artificial neural network and projection pursuit evaluation (PPE) have been developed for WRCC evaluation (Jiang et al. 2016; Sakaa et al. 2013). Each method has both advantages and disadvantages. The traditional evaluation method for determining the weight of factors has large subjectivity. The PPE model is fast, accurate, and objective to determine the weight of a nonlinear index. It has advantage of combining several optimization algorithms. The objective of the PPE model is to determine the optimum projection direction. Recently, the genetic algorithm (GA), improved genetic algorithm (IGA), and the swarm intelligence optimization algorithms, such as particle swarm optimization (PSO), firefly algorithm (FA), seeker optimization algorithm (SOA), and chicken swarm optimization (CSO) algorithms, have been widely used to optimize the projection direction in PPE model (Berro et al. 2010; Meng et al. 2014; Liu et al. 2018a; Liu et al. 2018b). These algorithms are mainly based on relatively simple concepts, which are easier to implement with respect to other methods, and avoid local optimums. The CSO is a global optimization algorithm based on chicken foraging behavior, which has a faster convergence rate and relatively robust performance. Since the CSO algorithm overcomes function optimization problems relative to GA, PSO, and FA algorithms, it has been widely used in the wireless internet network, cloud computing, mechanical engineering, and water systems (Li et al. 2017; Shayokh and Shin 2017; Liu et al. 2018a; Torabi and Safi-Esfahani 2018).

The main objective of this study is to develop a method for evaluating the WRCC by combining the CSO algorithm and a projection pursuit model. The CSO algorithm was validated using four typical function tests, and performance was compared with that of the PSO, FA, and SOA algorithms in terms of optimization. Based on the DPSIRM model, an index system including 20 indicators that were selected from the drivers, pressure, state, impact, response, and management subsystem was developed to evaluate the WRCC. An evaluation method was proposed to optimize the PPE model (CSO-PPE). The CSO-PPE and DPSIRM models were used to evaluate the WRCC of Shaanxi province between 2007 and 2016.

Material and methods

Study area and data

Shaanxi province lies in the northwest arid region of China (31.7° N–39.5° N, 105.5° E–111.2° E) (Fig. 1), which covers an area of 205,800 km^2. It has a continental monsoon climate, with annual average precipitation of 576.9 mm and annual average temperature of 13.0 °C. In 2016, the total amount of water resource was estimated at 27.15 billion m^3, and the per capita water resource was 713.91 m^3. The spatial and temporal distributions of precipitation are uneven with the annual precipitation gradually decreasing from south to north and 39 to 64% of annual total precipitation concentrates in the summer (Jiang et al. 2013).

Shaanxi province can be divided into southern Shaanxi, northern Shaanxi, and the Guanzhong plain according to the local administration. Southern Shaanxi lies in the Qinba mountain area and includes Hanzhong, Ankang, and Shangluo cities. The Han River and Jialing River in southern Shaanxi are important branches of Yangtze. It represents the middle line of the south-to-north water transfer project of the Water Conservation District, and thus eco-environmental protection must have priority but severely restrict the development of the local economy. The Guanzhong plain consists of five cities (Xi'an, Tongchuan, Baoji, Xianyang, and Weinan) and the Yangling ecological demonstration area, with nearly

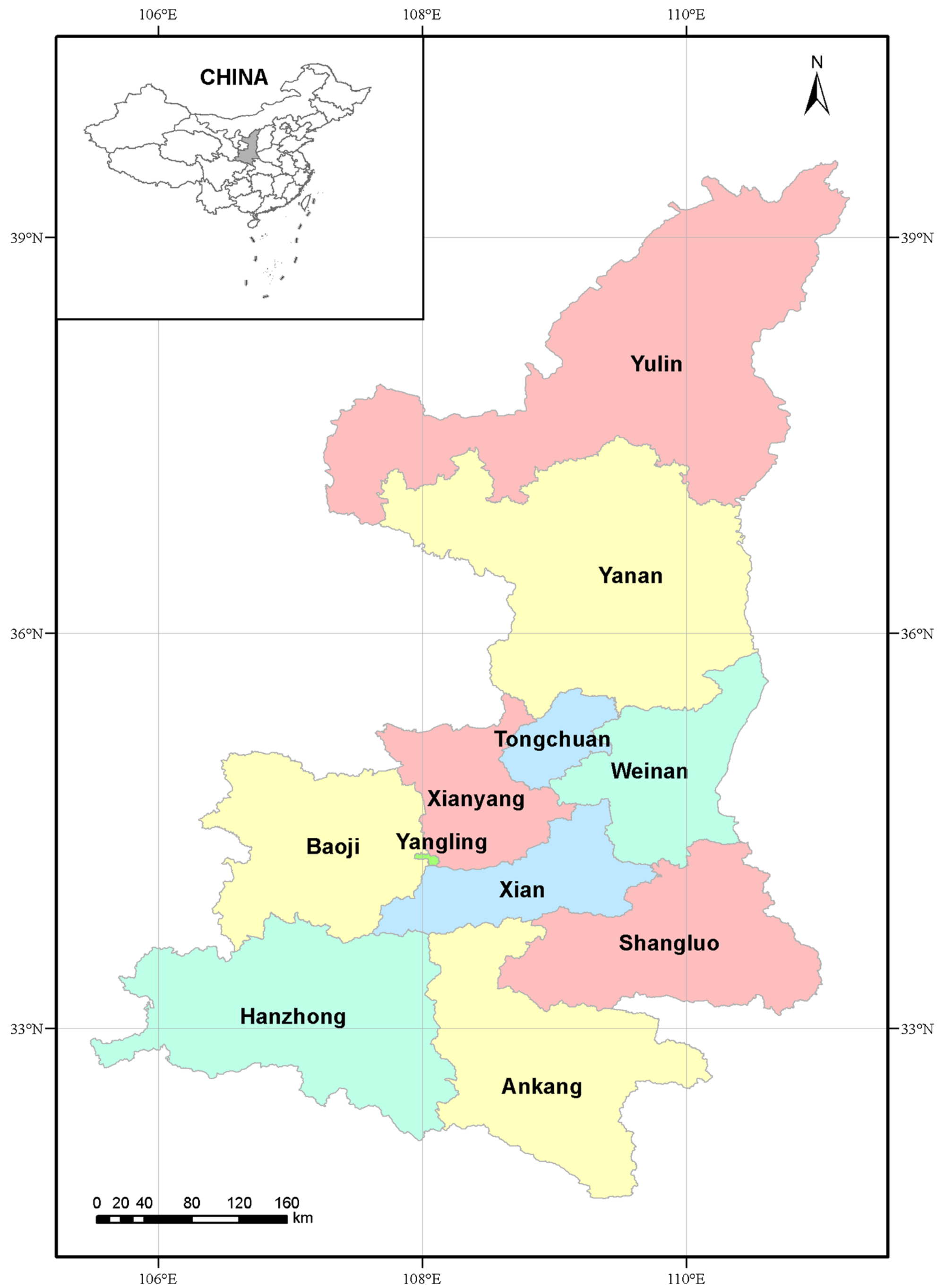

Fig. 1 Location of the study area

75% of the entire population of Shaanxi province. As the core economic region of Shaanxi province, water resource demand has consistently increased. Northern Shaanxi including Yulin and Yanan cities is dominated by deserts and the Loess Plateau. It is well-known for its deep loess deposits and high levels of soil erosion caused by droughts and semi-droughts in the arid climate and the special properties of loess (Jiang et al. 2017).

The data sets used in this study mainly included social, economic, environmental, and water resource utilization data. The social and economic data were obtained from the "Shaanxi Statistical Yearbook" (2008–2017) and the "Bulletin of National Economy and Social Development." Water resource utilization and environmental data were obtained from the "Shaanxi Water Resources Bulletin (2007–2016)" and the "Shaanxi Environmental Bulletin (2008–2017)."

DPSIRM model

The DPSIRM model was used to describe the water resource system, which was divided into six subsystems including the drivers, pressure, state, impact, response, and management subsystems. Figure 2 shows the DPSIRM framework of WRCC model. As driving factors of water resources change, the development of population, economy, and society are considered to represent the drivers subsystem. The pressure induced by water shortage and sewage discharge from these driving factors is used to represent the pressure subsystem. The high water demand and supply are considered to represent the state subsystem. The demand and supply contradictions lead to worsening relationships between humans and nature, which is then used to represent the impact subsystem. A series of measures used to treat the contradiction are considered to represent the response subsystem. Aiming to improve water resource utilization and decrease sewage discharge, policies and regulations have been implemented to increase WRCC and further the sustainable development of economy and society, which are considered to represent the management subsystem. Management is an effective way to alleviate the supply and demand contradiction of water resources. Thus, management affects the whole DPSIRM framework. The DPSIRM model was used to simulate the water resources-society-economy-ecological environment compound ecosystem. Thus, the interactions between water resources and the development of human society could be analyzed.

PPE model

Projection pursuit is a statistical method for high dimensional and non-normal data analysis. The basic principle of PPE is based on projects with high dimensional data being set to low dimensional subspace through computer techniques. By means of the optimizing projection function, a projection vector is obtained, which can reflect the structures and characters of the high dimensional dataset. The method can be used to analyze data in a low-dimensional space to research and analyze high dimensional data (Wang and Ni 2008). The steps for the PPE model were as follows:

Step 1: Normalization of sample index value. The evaluation sample set is defined as $\left\{x_{ij}^{*} \mid i=1,2,\ldots,m; j=1,2,\ldots,n\right\}$, where x_{ij}^{*} is the jth index value of the ith sample, m is the number of the sample, and n is the number of the index. To eliminate the dimension effect and unite the range of index value, the following formula was used to normalize the data:

$$x_{ij}=\begin{cases}\dfrac{x_{ij}^{*}}{x_{j\,max}} & positive\ index\\ \dfrac{x_{j\,min}}{x_{ij}^{*}} & negative\ index\end{cases} \tag{1}$$

where $x_{j\,max}$ and $x_{j\,min}$ are the maximum and minimum initial values of the *jth* index, and x_{ij} is the value list after normalization.

Step 2: Constructing the projection index function $Q(a)$. The projection pursuit method is a process of projecting the n dimensional data $\{x_{ij} | j=1,2,\ldots,n\}$ into the one dimensional projection value z_i based on the direction of $a=\{a_1,a_2,\ldots,a_n\}$.

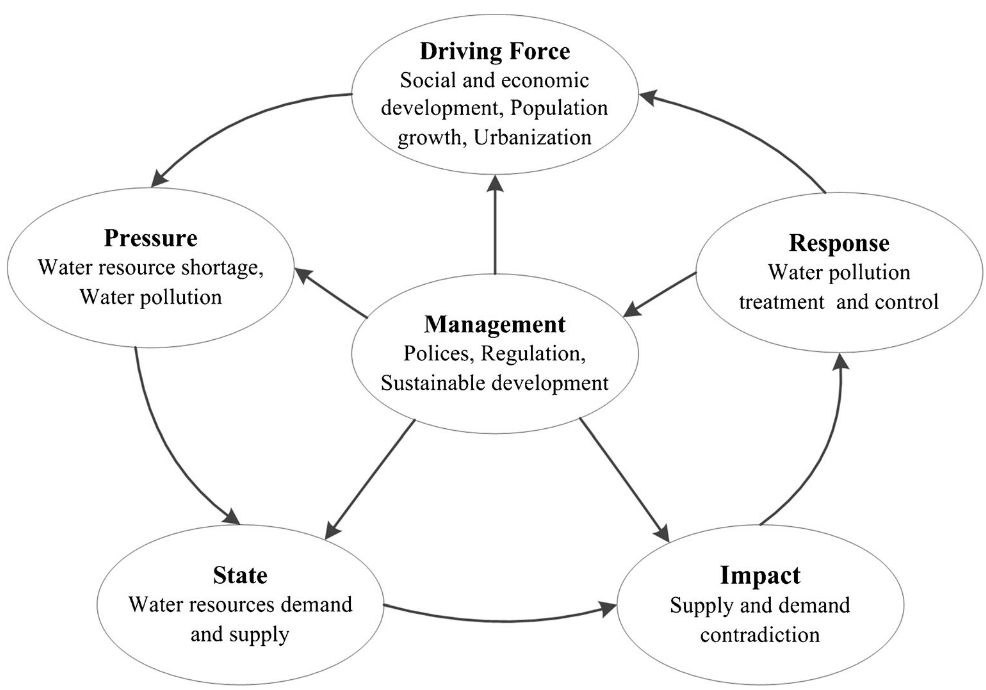

Fig. 2 The drivers-pressure-state-impact-response-management (DPSIRM) framework of WRCC model

$$z_i = \sum_{j=1}^{n} a_j x_{ij} (i = 1, 2, \ldots, m) \tag{2}$$

where a is the n-dimensional unit vector. The projection index function can be expressed as follow:

$$Q(a) = S_Z D_Z \tag{3}$$

where S_Z is the standard deviation of z_i (Eq. (4))and D_Z is the partial density of z_i (Eq. (5)).

$$S_Z = \sqrt{\frac{\sum_{i=1}^{m} (z_i - E_z)^2}{n-1}} \tag{4}$$

$$D_Z = \sum_{i=1}^{m} \sum_{j=1}^{n} (R - r_{ij}) u(R - r_{ij}) \tag{5}$$

where E_z is the average of series $\{z_i \mid i = 1, 2, \ldots, m\}$; R is the window radius of the partial density, commonly, $R = 0.1S_Z$; r_{ij} is the distance of the sample; and $r_{ij} = |z_i - z_j|$; $u(t)$ is the unit step function; when $t \geq 0$, $u(t) = 1$ and when $t < 0$, $u(t) = 0$.

Step 3: Optimizing the projection index function. When the sample set of indexes was fixed, the projection index function only changed with projection direction, which reflects the different characteristics of the data structure. The optimal direction of projection can maximize the characteristic structure of high dimensional data. Thus, we can estimate the optimal projection direction by determine the maximum of the projection index function (Eq. (6) and Eq. (7)).

$$Objective\ function : max\ Q(a) = S_Z D_Z \tag{6}$$

$$Constraints\ condition : s.t. : \sum_{j=1}^{n} a_j^2 = 1 \tag{7}$$

This is a complex optimization problem, in which $\{a_j \mid j = 1, 2, \ldots, n\}$ is the optimized variable.

Step 4: Comprehensive evaluation. The optimal projection direction a obtained from step 3 was input to Eq. (2). Then we obtained the projection value z_i^* of each sample. Higher z_i^* indicates higher WRCC.

CSO algorithm

The CSO algorithm is a swarm intelligence optimization method that simulates the social behavior of foraging chickens and has four main characteristics. First, there are multiple subgroups in a chicken swarm, and each subgroup comprises one dominant rooster and least one hen and a number of chicks. Secondly, individuals within the chicken swarm are divided according to fitness. The individuals with the highest fitness are defined as roosters, and each rooster leads a subgroup. The individuals with the lowest fitness are defined as chicks, and the remaining chickens are defined as hens. The hens and chicks randomly establish their mother-child relationship, and hens randomly choose subgroups to live. Thirdly, the affiliation, hierarchical order, and mother-child relationship remain constant once established in any subgroup. They are only updated during the iteration process. Finally, all individuals in a subgroup follow the rooster when foraging. Roosters have an advantage in competition for food followed by the hens and then the chicks.

A chicken swarm includes three types of chickens. Assume that D is the dimension of the foraging space, N is the number of chickens in the swarm, R is the number of roosters, H is the number of hens, and C is the number of chicks. The position update equation for individuals differs according to characteristics of the chicken swarm, and the roosters with the highest fitness have the broadest foraging range. The position x_{ij}^t $(i = 1, 2, \ldots, N; j = 1, 2, \ldots, D)$ indicates the value of the ith rooster in the jth dimension and the tth iteration. The position update equation in the $(t + 1)th$ iteration was as follows:

$$x_{ij}^{t+1} = x_{ij}^t \left(1 + randn\left(0, \sigma^2\right)\right) \tag{8}$$

when $f_i \leq f_k$, $\sigma^2 = 1$, otherwise, $\sigma^2 = exp\ ((f_k - f_i)/(|f_i| + \varepsilon))$,where ε is the smallest constant $(\varepsilon \neq 0)$; k is the rooster randomly chosen from the rooster group $(k \neq i)$; f_i and f_k are the fitness values of the ith rooster and jth rooster, respectively; $randn(0, \sigma^2)$ is the normal distribution of random numbers.

The position update equation of the ith hen in the jth dimension for the $(t + 1)th$ iteration was as follows:

$$x_{ij}^{t+1} = x_{ij}^t + S_1 rand\left(x_{rj}^t - x_{ij}^t\right) + S_2 rand\left(x_{sj}^t - x_{sj}^t\right) \tag{9}$$

where S_1 and S_2 are learning factors, $S_1 = exp\ ((f_i - f_r)/(|f_i| + \varepsilon))$, $S_2 = exp\ (f_s - f_i)$, $rand$ is a uniformly distributed random number over [0,1]. r is the rooster in the same subgroup as the ith hen, s is the individual randomly chosen from the roosters or hens $(r \neq s)$.

The position update equation of the ith chick in the jth dimension for the $(t + 1)th$ iteration was as follows:

$$x_{ij}^{t+1} = x_{ij}^t + F\left(x_{mj}^t - x_{ij}^t\right) \tag{10}$$

where m is the hen of the ith chick's mother; F is a uniformly distributed random number over [0,2].

CSO-PPE model

The calculation steps of CSO-PPE model were as follows:

Step 1: Data preprocessing. A normalization process for the data was performed with Eq. (1). Then we set the scale of chicken swarm as N; random parameters as F, and the maximum number of iterations as T.

Step 2: Rank order establishment. We established the rank order according to the four assumptions of the chicken swarm behavior, and then divided the chicken swarm into G groups and randomly established mother-child relationships with hens and chicks.

Step 3: Objective function confirmation. The CSO algorithm was applied to obtain the minimum value; thus, the reciprocal of Eq. (6) was used as the objective function and the Eq. (7) was used as the constraint condition in the following equation:

$$\begin{cases} min\ Q(a) = 1/(S_Z D_Z) \\ s.t.\ \sum_{j=1}^{n} a_j^2 = 1 \quad a_j \in [0,1] \end{cases} \tag{11}$$

Step 4: Initialization. We randomly initialized the position x_{ij}^t of chickens to calculate the fitness of the objective function using Eq. (11), and then selected the highest fitness value and its corresponding position.

Step 5: Iteration. When the randomly selected *ith* chicken was a rooster, hen, or chick, the position was updated using Eqs. (8), (9), and (10), respectively.

Step 6: Calculate fitness function. The fitness value calculated using Eq. (11) was used to update the position. If the updated fitness value was higher than the initial optimal fitness value, then we replaced the latter with the former. Otherwise individual positions were not replaced.

Step 7: Determine the optimal individual with the highest fitness and its position (i.e., the best projection direction a). Then we determined whether the termination condition of the algorithm met the demands. If it did meet the demand, then we moved on to step 8; otherwise, we repeated steps 4–7.

Step 8: Evaluation. The projection value z_i^* of each year was obtained from the best projection direction a and input to Eq. (2). According to the priority sequence of the projection value z_i^*, we evaluated the WRCC.

In the CSO-PPE model, the optimal projection direction of each component reflects the degree of influence each subsystem index. The greater value of projection direction, the greater effect on WRCC. The projection value z_i^* reflects the level of WRCC. The bigger projection value indicated higher WRCC and large exploitation potential. The smaller projection value indicated lower level of WRCC and little exploitation potential.

Results

Below the CSO, algorithm was firstly validated using four typical function tests to demonstrate the superiority of CSO, and then an index system based on the DPSIRM model was established. Finally, the CSO-PPE and DPSIRM models were used to assess the WRCC of Shaanxi province for the period of 2007–2016.

Comparative analysis between CSO and other three optimization algorithms

To evaluate the ability of the CSO algorithm, four typical test functions were selected to simulate and determine the minimum test function value (Table 1). Sphere and Rosenbrock are unimodal functions, which are used to test the convergence rate and optimization accuracy of algorithms. Schaffer and Rastrigin are multimodal functions with a large number of local extremes, which are used to test global optimization performance and ability to avoid precocious convergence. To compare the performance of four optimization algorithms, the same number of iterations ($T = 1000$) and population size ($M = 50$) were used. Other parameters of algorithms were as follows: PSO reduction coefficient, ω=0.99; local learning factor, $C1 = 2.0$; global learning factor, $C2 = 2.0$; maximum membership degree of the SOA algorithm, $u_{max} = 1.0$; minimum membership degree, $u_{min} = 0.0111$; maximum weight, $\omega_{max} = 0.9$; minimum weight, $\omega_{min} = 0.1$; maximum attraction degree of FA algorithm, $\beta_0 = 2.$; light intensity absorption coefficient, $\gamma = 1$; step factor, $\alpha = 0.2$; number of roosters in the CSO algorithm, $R = 0.3$ M; number of hens, $H = 0.6$ M; and number of chicks, $C = 0.1$ M.

Matlab was used for optimization calculation, which was repeated 30 times for four test functions. Evaluate FA, PSO, SOA, and CSO algorithms from two perspectives, the average values and the standard deviation. The average value reflected the solution precision that the algorithm achieved when running to the maximum number of iterations. The standard deviation reflected the convergence and stability of the algorithm. Table 2 shows the comparison of the optimization results for four algorithms. For Sphere, Schaffer, Rosenbrock, and Rastrigin functions, the optimal solution on average value and standard deviation were small (close to zero) based on the CSO algorithm.

Figure 3 shows the convergence curves for different algorithms. For the Schaffer and Rastrigin functions, the CSO algorithm gave the theoretical optimum value when iterated less than 250 times. These results suggest that the optimum speed and performance of the CSO algorithm were better than those of the FA, SOA, and PSO algorithms regarding unimodal and multimodal functions. The CSO algorithm has a strong ability and fast convergence speed to search for optimal values.

Table 1 Four typical test functions used in the CSO algorithm

Number	Function Name	Formula	The range of values	Theoretical optimal solution
1	Sphere	$f(x)=\sum_{i=1}^{N}x_i^2$	[− 100,100]	min f = 0
2	Rosenbrock	$f(x)=\sum_{i=1}^{N}\left[100\left(x_{i+1}-x_i^2\right)^2+\left(x_i-1\right)^2\right]$	[− 30,30]	min f = 0
3	Schaffer	$f(x,y)=0.5+\left(sin^2\sqrt{x^2+y^2}-0.5\right)/\left(1+0.001\left(x^2+y^2\right)^2\right)^2$	[− 10,10]	min f = 0
4	Rastrigin	$f(x)=\sum_{i=1}^{N}[x_i{}^2-10cos(2\pi x_i)+10]$	[−5.12,5.12]	min f = 0

The index system of WRCC in the DPSIRM framework

The index system was developed to be comprehensive, practical, representative, and easily to operate. We combined the actual conditions from the Shaanxi province to design an evaluation index system for WRCC based on DPSIRM model. Twenty indicators from six subsystems were selected for the evaluation of WRCC. The indices were divided into two types, positive and negative index. Higher positive index along with lower negative index represent higher WRCC, and lower positive index along with higher negative index represent higher WRCC. Table 3 shows the connotation, type, and units of indices of WRCC.

The evaluation results of WRCC using the CSO-PPE model

The projection index function for the normalization data for the period of 2007–2016 was constructed according to the CSO-PPE model. The optimal projection direction with the CSO algorithm was used to solve the PPE model function. The CSO algorithm searching scope was set within [0, 1]. The CSO algorithm was run 20 times to calculate the averages of best projection direction a = [0.2413, 0.0879, 0.0965, 0.2758, 0.1840, 0.1973, 0.3206, 0.2038, 0.1276, 0.2487, 0.2304, 0.1851, 0.2299, 0.1624, 0.3147, 0.2128, 0.2569, 0.3324, 0.1924, 0.1703]. The projection value z_i^* of Shaanxi province and each city were calculated by substituting the best projection direction a into Eq. (3). The evaluation results were analyzed based on the projection values.

Discussion

Analysis of DPSIRM subsystem of WRCC in Shaanxi Province

Figure 4 shows that the relative impact from the pressure subsystem was 22.34%, indicating that this is the most important factor that influences the WRCC of Shaanxi province. Five indicators including the share of GDP invested in environmental pollution control (M1), total volume of discharged wastewater (P4), the reaching standard rate of treated industrial waste water (R1), water consumption per 10,000 yuan (P1), and utilization ratio of water resources (R3) greatly affect the WRCC. Considering the current situation of water resources, environment, and socioeconomic conditions in Shaanxi province, water resource planning and management should consider the following points. Firstly, the GDP invested in environmental pollution control reflects the degree of environmental governance investment. The water consumption and wastewater discharge increase continuously in Shaanxi province, which resulted in shortages of water resources and severe environmental pollution. Investment in environmental protection has roughly tripled compared with that in 2007. Thus, increasing investment in water pollution is an effective way to resolve water resource shortages. Secondly, the discharged wastewater and the reaching standard rate of treated industrial wastewater have greatly influenced the availability of water resources. Many industrial discharges into water bodies have caused

Table 2 Comparison of the optimization results for four algorithms

Function	Algorithm	Average value	Standard deviation	Function	Algorithm	Average value	Standard deviation
Sphere	SOA	1.14E-04	5.19E-05	Schaffer	SOA	4.06E-08	5.26E-08
	PSO	2.82E-03	1.14E-03		PSO	3.33E-06	3.29E-06
	FA	6.46E-05	1.54E-04		FA	1.46E-08	1.05E-10
	CSO	9.15E-60	2.24E-59		CSO	0	0
Rosenbrock	SOA	1.87E-06	1.45E-06	Rastrigin	SOA	7.43E-06	6.48E-06
	PSO	2.27E-03	1.89E-03		PSO	8.48E-04	6.18E-04
	FA	8.72E-06	1.27E-05		FA	3.20E-06	1.38E-06
	CSO	0	0		CSO	0	0

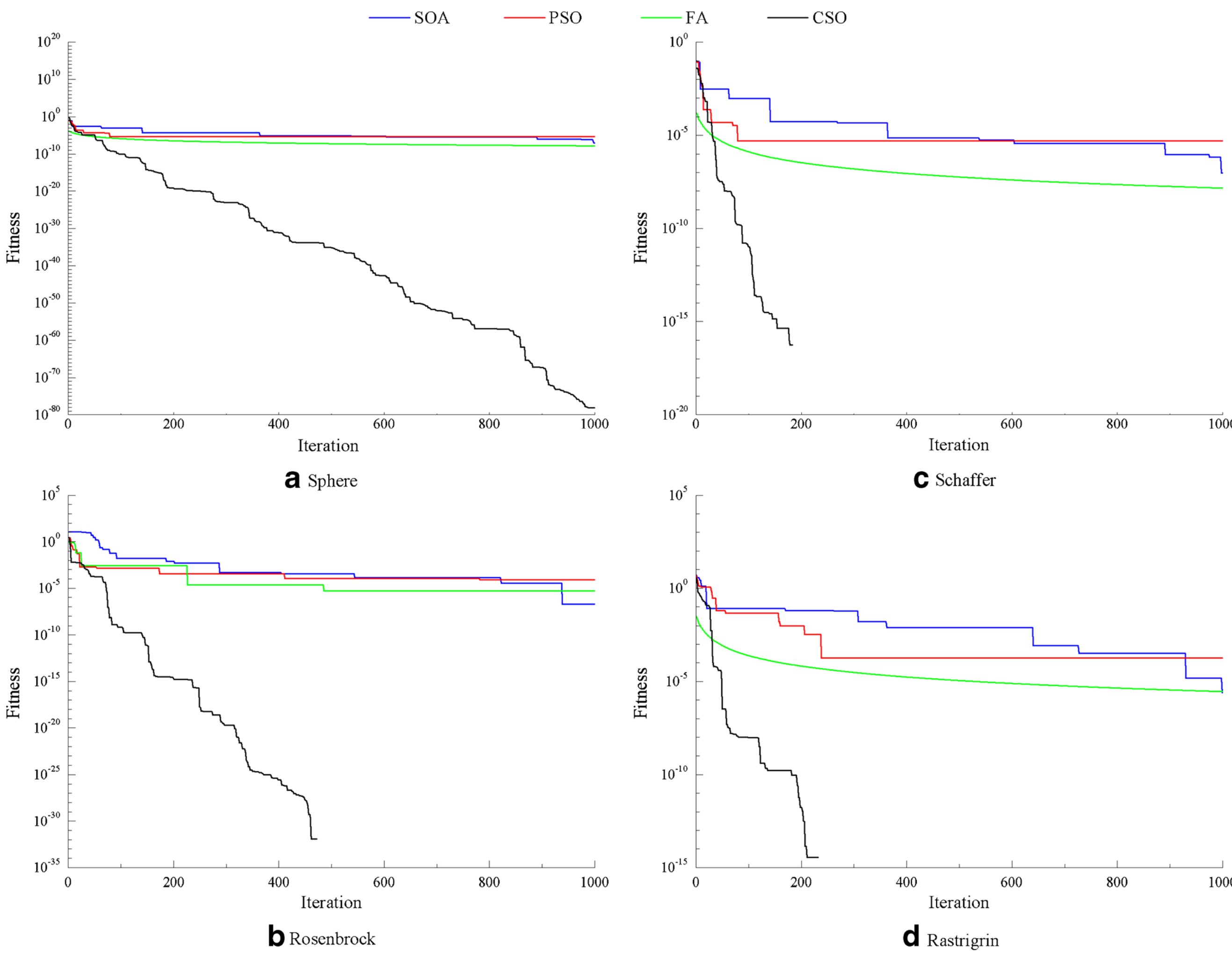

Fig. 3 Comparison of the convergence curves for SOA, PSO, FA, and CSO algorithm for four functions. **a** Sphere. **b** Rosenbrock. **c** Schaffer. **d** Rastrigrin

deterioration in water quality. The water resources quantity may not be decreasing. However, the amount of usable water had declined. This leads to water shortages and decreased water quality, which decreases the level of WRCC

Water consumption per 10,000 yuan indicated the effect of economic activities on WRCC. Contradictions between water supply and demand will be more serious with future social and economic development. The reasonable collocation and optimized scheduling of water resources will solve these contradictions. Finally, the utilization ratio of water resources reveals the present situation and utilization of water resources. Utilization of regional water resources has exceeded carrying capacity, causing environment deterioration. Therefore, effectively increasing water utilization efficiency and establishing a water-saving society have become urgent objectives to solve regional water conflict issues.

Figure 5 shows that the relative influence of drivers and the pressure subsystem on WRCC has gradually increased. In 2016, the proportion of drivers and pressure subsystem increased 1.3 times with respect to that of 2007. The results indicate that socioeconomic development plays an important role in WRCC increases, and the pressure from water demand in this area consistently increases. The influence of the management subsystem slightly increased to reflect the management of water resources, which plays an active role in WRCC increases. The WRCC of Shaanxi province had increase from 2007 to 2016. Under the current socioeconomic conditions, the available water resources can support both the ecological environment and sustainable development. However, the WRCC decreased in 2008. The data shows that precipitation decreased by 9.8% compared with the average annual precipitation, and total water resources reduced by 28.2% on average. Therefore, Shaanxi province was short of water resources in 2008. The WRCC increases slowed down from 2011 to 2016. However, its level was still relatively high. Shaanxi province began to implement the strictest water resource management system in 2011, including three aspects (water intake, water use, and water drainage). Thus, a system related to the above three aspects and water management was developed to promote water saving, protection, and utilization efficiency.

Table 3 The index system of WRCC

Subsystem	Indices	Units	Connotation	Type
Driver force (D)	Per capita GDP (D1)	CNY/person	The driving effect of economy development	Positive
	Population density (D2)	person/km^2	The driving effect of population density	Negative
	Urbanization rate (D3)	%	The driving effect of regional development	Positive
Pressure (P)	Water consumption per 10,000 yuan (P1)	m^3/10^4 CNY	The pressure of water quantity from economic development.	Negative
	Water consumption per 10,000 yuan of value-added by agriculture (P2)	m^3/10^4 CNY	The pressure of water quantity from agricultural water.	Negative
	Water consumption per 10,000 yuan of value added by industry (P3)	m^3/10^4 CNY	The pressure of water quantity from industrial water.	Negative
	Total volume of waste water discharged (P4)	10^9 ton	The pressure of water quality from production and living.	Negative
State (S)	Per capita water resources (S1)	m^3/person	The per capita state of water resources	Positive
	Per capita cultivated land area (S2)	hm^2/person	The state of regional environment	Positive
	Per unit area water resources (S3)	10^4 m^3/km^2	The per unit area state of water resources	Positive
	Annual precipitation (S4)	10^9 m^3	The natural state of water resources	Positive
Impact (I)	Areas affected by drought and flood (I1)	10^4 hm^2	The impact of climate change on water resources	Negative
	Energy consumption per unit of GDP (I2)	tce/10^4 CNY	The impact of resource utilization on water resources	Negative
	Forest coverage rate (I3)	%	The impact of water storage capacity on water resources	Positive
Response (R)	The reaching standard rate of treated industrial waste water (R1)	%	The response of safety of water quality	Positive
	Sewage treatment rate (R2)	%	The response of safety of water quality	Positive
	Utilization ratio of water resources (R3)	%	The response of safety of water quantity	Negative
Management (M)	The share of GDP invested in environmental pollution control (M1)	%	Reflect the investment of environmental protection and management	Positive
	Green coverage rate of built-up areas (M2)	%	Reflect the construction and management of ecological environment	Positive
	Area of soil and water conservation (M3)	10^{4}hm^2	Reflect the control of soil and water loss	Positive

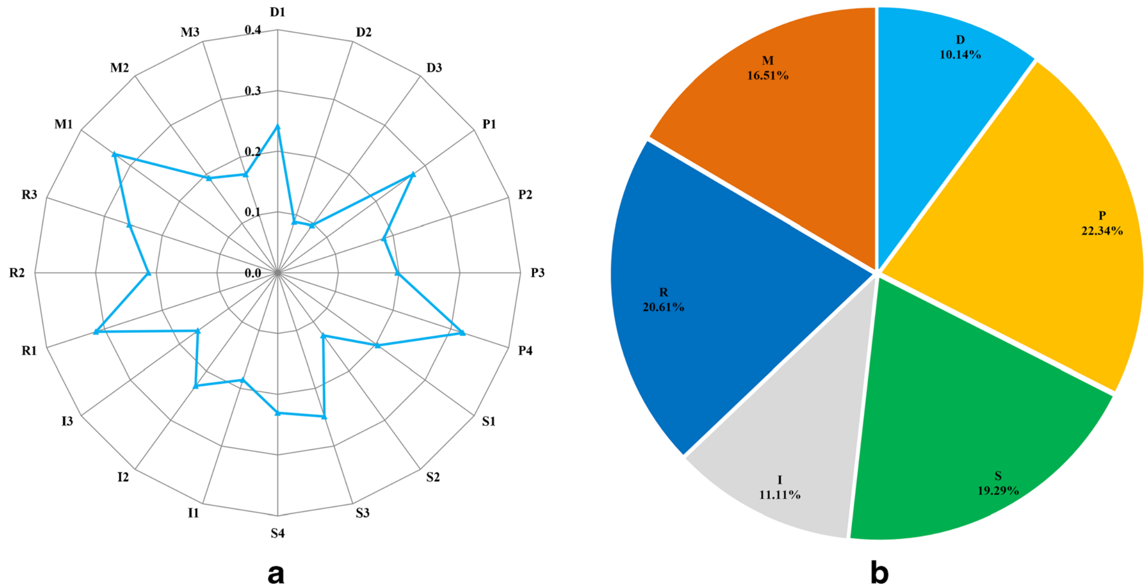

Fig. 4 **a** The optimal projection direction of each index. **b** The proportion of each subsystem impact

Spatial-temporal variations of WRCC in Shaanxi Province

The aim of WRCC evaluation in each city was to reveal regional differences. It was the effective way to improve the carrying capacity of water resources in Shaanxi province from the perspective of regional coordination. The initial data from 11 cities were subjected to the normalization process using the Eq. (1), and the projection values z_i^* were determined using the best projection direction a. The projection values were used to analyze the results of WRCC (Figs. 6 and 7).

Figure 6 shows that the WRCC of Shaanxi province and 11 cities gradually increased over the period of time investigated with social and economic development. However, the average

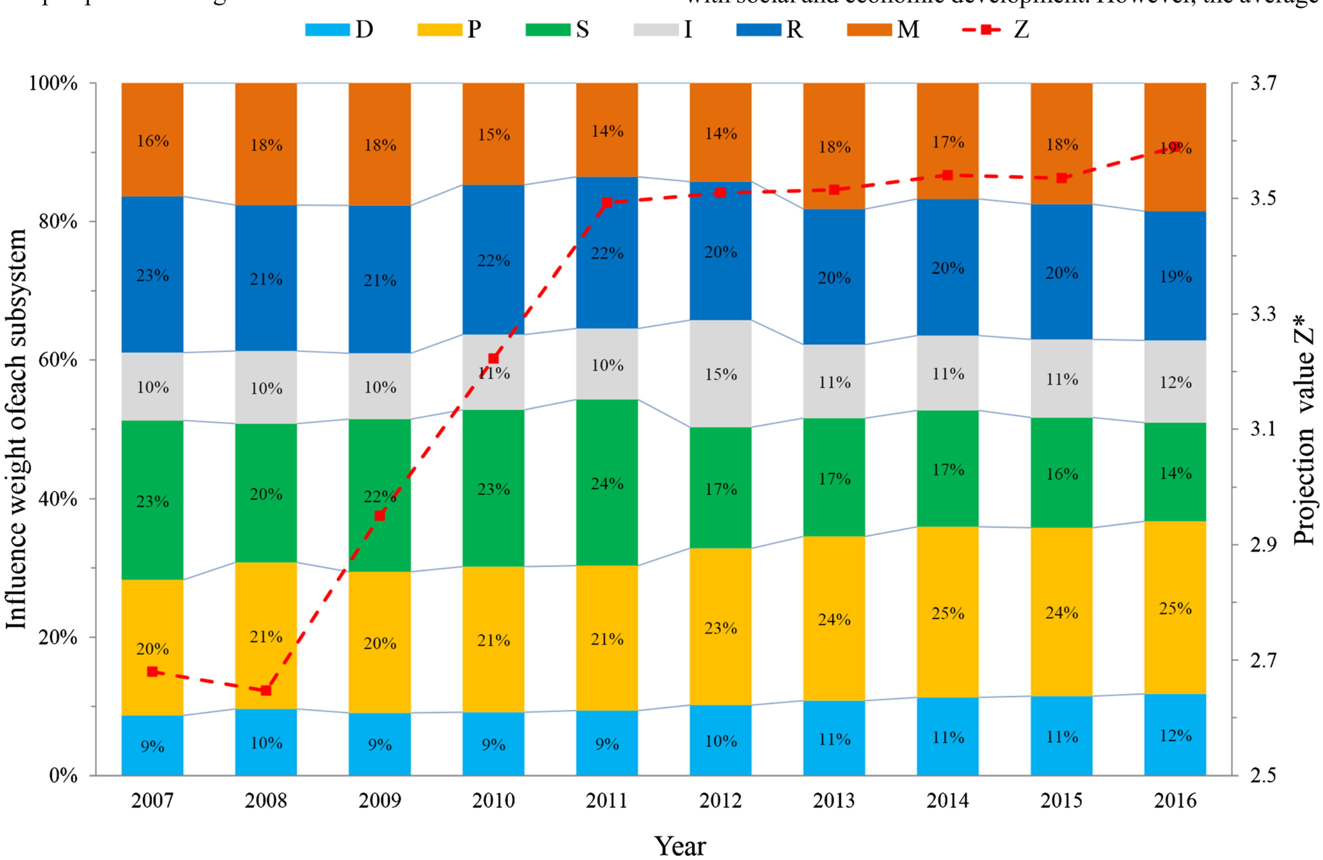

Fig. 5 Cumulative percentage of DPSIRM subsystem and the projection value (red dashed line)

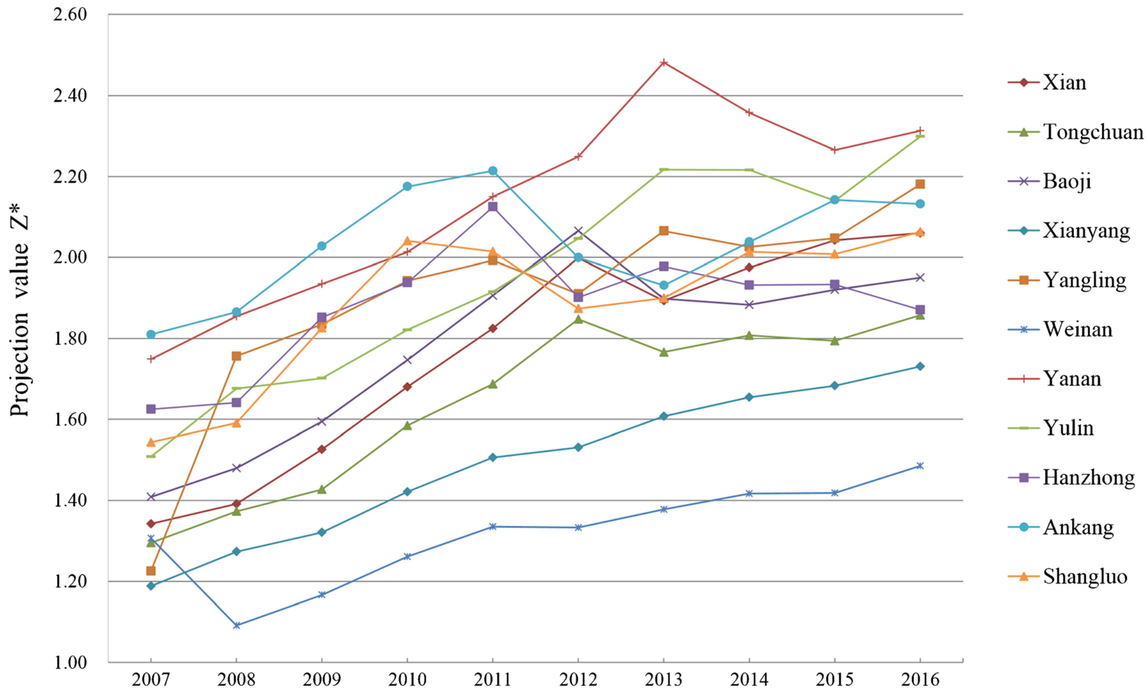

Fig. 6 The trends in the projection value of each city in Shaanxi province

projection value of WRCC was only 1.8 and at a lower level. This was possibly because the population pressure in Shaanxi province was enormous. The average population density of Shaanxi province was 182 people per km^2, with a much higher density than that of the country average (140 persons per km^2). Moreover, a lack of water saving activities increased the pressure on water resources. Then, the water resources were overly scarce in Shaanxi province.

Precipitation and its spatial and temporal distribution are uneven in this area. Therefore, there are distinct wet and dry seasons, and there are different water resources in different cities. Per capita water resources in Shaanxi province was about 1042 m^3. According to international standards, per capita water resources less than 2000 m^3 represents moderate water shortage. These factors influenced the WRCC. Lastly, the distribution of industries in Shaanxi province was uneven. The proportions of primary, secondary, and tertiary industries were 9, 49, and 42%, respectively. The proportions of the primary and secondary industries were slightly higher than the national average. Besides, agricultural and industrial water accounted for 52 and 15% of the total water consumption, respectively, and they were major water consumers. Optimizing and adjusting industrial structures is of urgent necessity to decrease the stress caused by excessive water consumption.

Figure 7 shows that southern and northern Shaanxi had higher carrying capacity compared with that of Guanzhong region. The evaluation results of WRCC for Yanan, Ankang, Yulin, Yangling, and Shangluo cities were higher than the total mean value. Other cities had lower evaluation results than the total mean value, with the lowest projection value in Weinan city (1.3193). Though the total water resources were relatively scarce in northern Shaanxi, the WRCC of Yanan city ranked first in Shaanxi province, and Yulin city ranked third because of low population density. Owing to the vulnerable ecological environment of northern Shaanxi and the huge amounts of sewage discharge that are inefficiently treated and recycled, sewage treatment methods need to be improved to deal with water crises. As the water source area of the middle route project for south-to-north water transfer in Shaanxi province, southern Shaanxi was the abundant in water resources, with healthy ecosystem environment. Therefore, the WRCC of Ankang, Shangluo, and Hanzhong cities were much better. The water resources condition of Guanzhong region was uneven. Baoji, Xian, and Yangling cities were rich in water resources, but Tongchuan, Xianyang, and Weinan cities were poor. Guanzhong region is more socioeconomically developed but has a dense population and was also short of water resources. There was intense pressure on water resources from both residential and industrial parts of the urban areas. Especially in Weinan city that has the lowest WRCC for some time. Thus, it is vital to resolve the water resource problem in Weinan city.

Conclusions

This study proposed a CSO-PPE model to assess the WRCC in Shaanxi province. Based on the DPSIRM model and considering the economy, society, environment, and ecology, 20 indicators were selected to establish an evaluation index system for WRCC. By comparing and analyzing the optimization results of PSO, FA, and SOA, the CSO algorithm had a strong searching ability and fast convergence speed and provided

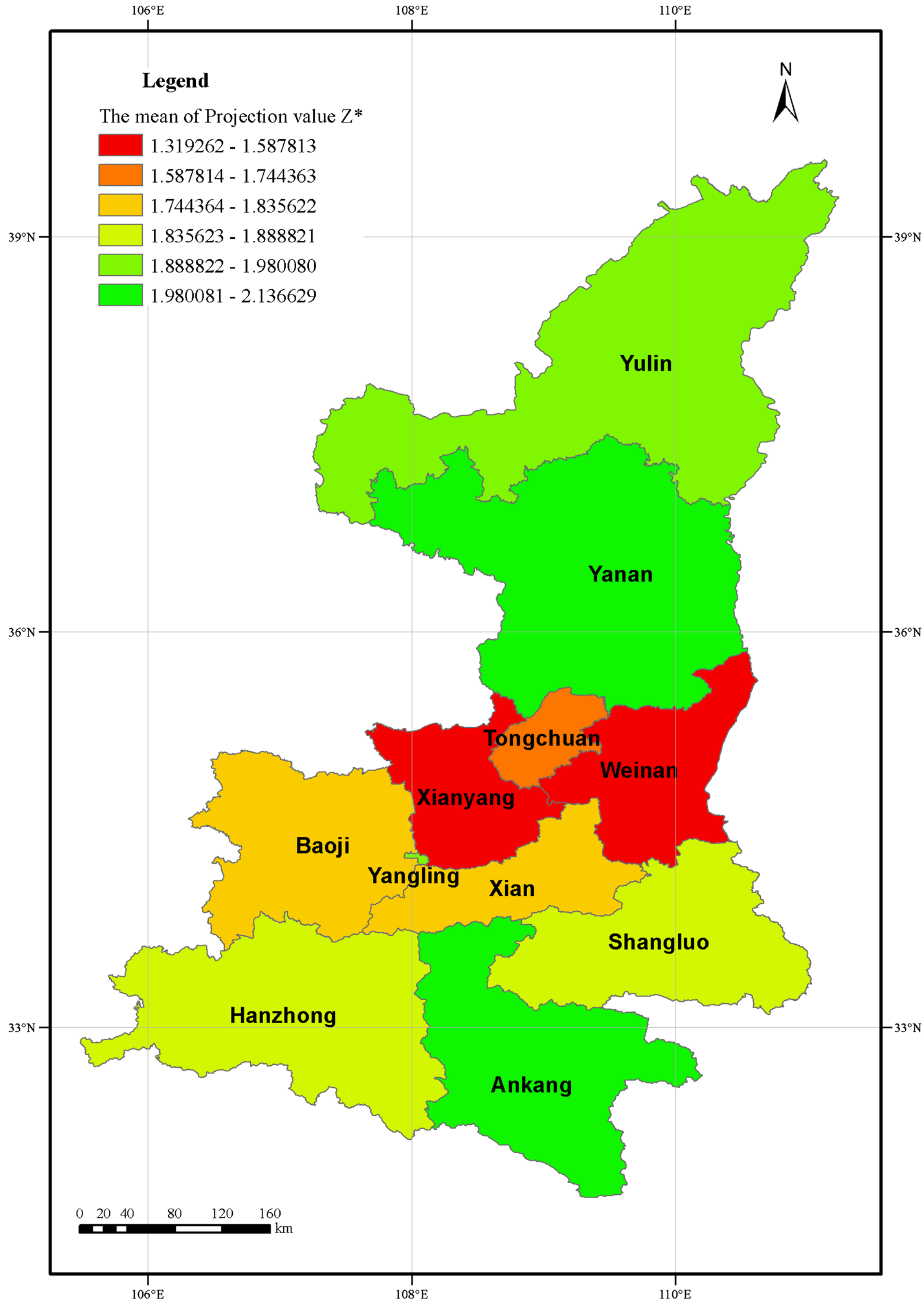

Fig. 7 The spatial distributions of the mean projection values of WRCC over the period 2007 to 2016

more accurate and stable optimal values. The CSO-PPE model can obtain the optimal projection direction and then objectively determine the degree to which different factors affect WRCC.

The results of the WRCC in Shaanxi province are consistent with the current situation. Hence, assessing each subsystem enables us to discover further problems in Shaanxi province over past several years, which could provide a scientific theoretical basis for water resource management. In addition, Shaanxi province should increase the WRCC in the future, by increasing awareness of water saving techniques, adjusting industrial structures, decreasing industrial and agricultural water consumption, increasing water utilization efficiency and pollution control, and decreasing soil water loss. In conclusion, the CSO-PPE evaluation method based on the DPSIRM model is a feasible and effective method to determine the WRCC, and the index system is a reasonable and scientific way to evaluate regional WRCC.

However, our study still has some limitations, such as discrepancies in the statistical standards used to generate the original data and relatively short time period investigated. Thus, our future research should focus on more specific indicator data, which will hopefully improve the accuracy of evaluation results.

Funding information This study was partly supported by the National Key Research and Development Program of China (2016YFC0401409), National Natural Science Foundation of China (51679188, 51509201, 51979221), and Natural Science Basic Research Plan in Shaanxi Province of China (2018JM5031).

Compliance with ethical standards

Conflict of interest The authors declare that they have no conflict of interest.

References

Berro A, Larabi Marie-Sainte S, Ruiz-Gazen A (2010) Genetic algorithms and particle swarm optimization for exploratory projection pursuit. Ann Math Artif Intell 60:153–178. https://doi.org/10.1007/s10472-010-9211-0

Clarke AL (2002) Assessing the carrying capacity of the Florida Keys. Popul Environ 23:405–418. https://doi.org/10.1023/a:1014576803251

Cook C, Bakker K (2012) Water security: debating an emerging paradigm. Glob Environ Chang 22:94–102. https://doi.org/10.1016/j.gloenvcha.2011.10.011

Daily GC, Ehrlich PR (1994) Population, sustainability, and earth's carrying capacity. Ecosystem Management:435–450. https://doi.org/10.1007/978-1-4612-4018-1_32

Feng LH, Zhang XC, Luo GY (2008) Application of system dynamics in analyzing the carrying capacity of water resources in Yiwu City, China. Math Comput Simul 79:269–278. https://doi.org/10.1016/j.matcom.2007.11.018

Gong L, Jin C (2009) Fuzzy comprehensive evaluation for carrying capacity of regional water resources. Water Resour Manag 23:2505–2513. https://doi.org/10.1007/s11269-008-9393-y

Graymore MLM, Sipe NG, Rickson RE (2010) Sustaining human carrying capacity: a tool for regional sustainability assessment. Ecol Econ 69:459–468. https://doi.org/10.1016/j.ecolecon.2009.08.016

Guo Q, Wang J, Yin H, Zhang G (2018) A comprehensive evaluation model of regional atmospheric environment carrying capacity: model development and a case study in China. Ecol Indic 91:259–267. https://doi.org/10.1016/j.ecolind.2018.03.059

Han Y, Wei F, Ye G, Yang S, Ma P, Hu W (2018) A study on evaluation the marine carrying capacity in Guangxi Province, China. Mar Policy 91:66–74. https://doi.org/10.1016/j.marpol.2018.02.003

Harris JM, Kennedy S (1999) Carrying capacity in agriculture: global and regional issues. Ecol Econ 29:443–461. https://doi.org/10.1016/S0921-8009(98)00089-5

Jiang R, Xie J, Li J (2013) Application of world wind on hydrologic monitoring and simulation in Shaanxi province, China. Disaster Advance 6:33–47

Jiang R, Xie J, He H, Luo J, Zhu J (2015) Use of four drought indices for evaluating drought characteristics under climate change in Shaanxi, China: 1951–2012. Nat Hazards 75:2885–2903. https://doi.org/10.1007/s11069-014-1468-x

Jiang R, Xie J, Xie J, He H, Kuo CC, Zhu J, Yang M (2016) Spatiotemporal variability and predictability of normalized difference vegetation index (NDVI) in Alberta, Canada. Int J Biometeorol 60:1389–1403. https://doi.org/10.1007/s00484-015-1132-5

Jiang R, Xie J, Zhao Y, He H, He G (2017) Spatiotemporal variability of extreme precipitation in Shaanxi province under climate change. Theor Appl Climatol 130:831–845. https://doi.org/10.1007/s00704-016-1910-y

Jiang R, Yu X, Xie J, Zhao Y, Li F, Yang M (2018) Recent changes in daily climate extremes in a serious water shortage metropolitan region, a case study in Jing-Jin-Ji of China. Theor Appl Climatol, 134: 565–584. doi: 10.1007_s00704-017-2293-4

Jiang R, Wang Y, Xie J, Zhao Y, Li F, Wang X (2019) Assessment of extreme precipitation events and their teleconnections to El Niño Southern Oscillation, a case study in the Wei River Basin of China. Atmos Res 218:372–384. https://doi.org/10.1016/j.atmosres.2018.12.015

Lane M (2010) The carrying capacity imperative: assessing regional carrying capacity methodologies for sustainable land-use planning. Land Use Policy 27:1038–1045. https://doi.org/10.1016/j.landusepol.2010.01.006

Li W, Jiang R, Zhao Y, Xie J, Zhu J, Cao R (2019) Water ecological environment protection under changing environment: a systematic review and bibliometric analysis. J Coast Res 93:9–15. https://doi.org/10.2112/SI93-002.1

Li Y, Wu Y, Qu X (2017) Chicken swarm-based method for ascent trajectory optimization of hypersonic vehicles. J Aerosp Eng 30: 04017043. https://doi.org/10.1061/(ASCE)AS.1943-5525.0000757

Liu D, Liu C, Fu Q, Li T, Khan MI, Cui S, Faiz MA (2018a) Projection pursuit evaluation model of regional surface water environment based on improved chicken swarm optimization algorithm. Water Resour Manag 32:1325–1342. https://doi.org/10.1007/s11269-017-1872-6

Liu D, Mu R, Fu Q, Liu C, Li T, Khan MI, Cui S, Faiz MA (2018b) An evaluation of the resilience of the regional agricultural water and soil resource system in Heilongjiang Province, China. Agricultural Research 7:311–320. https://doi.org/10.1007/s40003-018-0312-z

Mei H, Liuyuan, Duhuan, Yangxiaoyan (2010) Advances in study on water resources carrying capacity in China. Procedia Environ Sci 2:1894–1903. https://doi.org/10.1016/j.proenv.2010.10.201

Meng X, Liu Y, Gao X, Zhang HA (2014) New bio-inspired algorithm: chicken swarm optimization. Advances in Swarm Intelligence. Springer international Publishing 86-94. doi: https://doi.org/10.1007/978-3-319-11857-4_10

Min D, Zhenghe X, Limin P, Yunhai Z, Xiufeng X (2011) Comprehensive evaluation of water resources carrying capacity of Jining City. Energy Procedia 5:1654–1659. https://doi.org/10.1016/j.egypro.2011.03.282

Ren C, Guo P, Li M, Li R (2016) An innovative method for water resources carrying capacity research – metabolic theory of regional water resources. J Environ Manag 167:139–146. https://doi.org/10.1016/j.jenvman.2015.11.033

Rijsberman MA, Van de Ven FHM (2000) Different approaches to assessment of design and management of sustainable urban water systems. Environ Impact Assess Rev 20:333–345. https://doi.org/10.1016/S0195-9255(00)00045-7

Rouillard J, Vidaurre R, Brouwer S, Damman S, Ponce AA, Gerner NV, Riegels N, Termes M (2016) Governance regime factors conducive to innovation uptake in urban water management: experiences from Europe. Water 8:477. https://doi.org/10.3390/w8100477

Sakaa B, Chaffai H, Hani A (2013) The use of artificial neural networks in the modeling of socioeconomic category of integrated water resources management (case study: Saf-Saf river basin, north east of Algeria). Arab J Geosci 6:3969–3978. https://doi.org/10.1007/s12517-012-0654-y

Shayokh MA, Shin SY (2017) Bio inspired distributed WSN localization based on chicken swarm optimization. Wirel Pers Commun 97:5691–5706. https://doi.org/10.1007/s11277-017-4803-1

Sun S, Wang Y, Liu J, Cai H, Wu P, Geng Q, Xu L (2016) Sustainability assessment of regional water resources under the DPSIR framework. J Hydrol 532:140–148. https://doi.org/10.1016/j.jhydrol.2015.11.028

Torabi S, Safi-Esfahani F (2018) A dynamic task scheduling framework based on chicken swarm and improved raven roosting optimization methods in cloud computing. J Supercomput 74:2581–2626. https://doi.org/10.1007/s11227-018-2291-z

Varis O, Keskinen M, Kummu M (2017) Four dimensions of water security with a case of the indirect role of water in global food security. Water Security 1:36–45. https://doi.org/10.1016/j.wasec.2017.06.002

Wang SJ, Ni CJ (2008) Application of projection pursuit dynamic cluster model in regional partition of water resources in China. Water Resour Manag 22:1421–1429. https://doi.org/10.1007/s11269-007-9234-4

Wei Y, Huang C, Lam PTI, Yuan Z (2015) Sustainable urban development: a review on urban carrying capacity assessment. Habitat International 46:64–71. https://doi.org/10.1016/j.habitatint.2014.10.015

Xing Z, Qu R, Zhao Y et al (2019) Identifying the release history of a groundwater contaminant source based on an ensemble surrogate model. J Hydrol 572:501–516. https://doi.org/10.1016/j.jhydrol.2019.03.020

Yu DL, Mao HY (2002) Regional carrying capacity: case studies of Bohai Rim area. J Geogr Sci 12:177–185. https://doi.org/10.1007/bf02837472

Zhang F, Zhang J, Wu R, Ma Q, Yang J (2016) Ecosystem health assessment based on DPSIRM framework and health distance model in Nansi Lake, China. Stoch Env Res Risk A 30:1235–1247. https://doi.org/10.1007/s00477-015-1109-2

Zhang F, Liu X, Zhang J, Wu R, Ma Q, Chen Y (2017) Ecological vulnerability assessment based on multi-sources data and SD model in Yinma River Basin, China. Ecol Model 349:41–50. https://doi.org/10.1016/j.ecolmodel.2017.01.016